Multi-Objective Genetic Algorithm Optimization of Antennas for use in LWA

Aaron Kerkhoff, Applied Research Labs, University of Texas, Austin

11/11/2006

I. Introduction

Many of the technical requirements proposed for the LWA are significantly expanded compared with the LWDA. Among the most significant changes in requirements is the wider operating band of the LWA, nominally 20 MHz to 80 MHz [1], compared with 60 MHz to 80 MHz for the LWDA. This presents new challenges in designing many of the system components including the antenna. Requirements for an LWA antenna include good impedance matching and high radiation efficiency to enable sky noise limited operation in the receiver. The antenna must also exhibit wide beamwidth and omni-directional radiation patterns with low axial ratio circular polarization. All of these characteristics must be maintained over the full 20 MHz to 80 MHz operating band. Additionally, the antenna should be mechanically robust to withstand long-term field operations. Of course, the performance characteristics must be traded against the cost of the antenna which must be low in order to achieve a low station cost.

An effort is discussed in this document in which multi-objective genetic algorithm optimization is applied to the design of antennas for use in LWA. First, some background information is provided in the area of multi-objective optimization, and a Pareto-based genetic algorithm (GA) optimization code developed by ARL:UT is briefly discussed. A new simulation code, which can be used for the efficient analysis of planar antennas is described and its performance is compared against other simulation codes and measurement results. Recent results of applying the Pareto GA optimizer coupled with this antenna simulation code to the design of planar (or "blade"-like) dipoles for use in LWA are presented. Finally, upcoming work involving the Pareto GA optimizer is discussed.

Planar dipole antennas were selected for initial study with the Pareto GA optimizer since this type of antenna was used in LWDA, and scaled versions of the LWDA antenna have been considered for use in LWA. As a result, a good amount of reference data is already available for this type of antenna in order to rate the performance of the optimizer. Additionally, it is believed that compared with simpler antenna structures consisting of wire or tubular elements, planar dipoles bound the electromagnetic performance that can be achieved in a dipole antenna for LWA. Therefore, the results yielded from optimization of planar dipoles should be useful in judging the relative quality of other types of antennas considered for LWA as well. The optimizer may also be equally well applied to wire or tube based antennas. Therefore, follow-up studies to the planar dipole study could involve such antenna types as they are identified in the LWA effort.

II. Optimization Background

Global optimization schemes have received much attention recently in many areas of engineering including antenna design. Optimization approaches such as genetic

algorithms, simulated annealing, and particle swarm are capable of efficiently searching a design space to find a global optimum as compared with traditional, gradient based optimizers, which generally find local optima. Furthermore, these optimization schemes are robust to problems involving multiple objectives and many design parameters. These characteristics make the use of a global optimization approach attractive for the LWA antenna design problem which is fraught with numerous potential performance and cost trade-offs.

Our previous work in this area mostly involves applying traditional genetic algorithm (GA) optimizers to the design of planar monopole antennas. In [2], GA was used to study the trade-off that can be achieved between bandwidth and size with planar monopoles by varying the shape of radiating element. In this study, the impedance matching over a specified operating band was optimized for varying element size constraints. In [3], GA was used to improve the performance of a planar monopole for use with ultra-wideband communications having a narrow frequency notch in the operating band to mitigate interference with other in-band radio systems. Both impedance matching and radiation patterns were optimized over the wide operating band and the narrow notch band using a weighted (scalar) cost function approach.

While traditional GA optimizers can be used for multi-objective design problems, the need to select the proper weighting between different objectives in order to achieve the desired results is often problematic. Since the population of a traditional GA will converge towards a single optimal design, it is necessary to re-run the GA multiple times using different weightings in order to explore the available trade-offs between different objectives. A more efficient approach is to use a Pareto-based multi-objective GA [4] (here called the Pareto GA.) In contrast to a traditional GA, a Pareto GA spreads its population over the objective space in order to simultaneously explore different performance trade-offs. Through iteration of the optimizer, the population converges toward a Pareto front, which describes a near-optimal trade-off between different objectives over a wide range of objective values. This essentially provides a design curve by which one can select the desired trade-off.

We have developed a Pareto Multi-Objective GA optimization code specifically tailored for antenna design. At the heart of the code is a typical GA optimizer which can use various forms of selection, cross-over, and mutation to evolve the design population. A non-dominance ranking scheme has been added to the GA to enable Pareto multi-objective optimization. A sharing scheme is also used to maintain diversity over the Pareto front. Any number of design parameters can be included, which are generally encoded as binary strings for use in the GA; constraints can be placed on each parameter individually. Any number of objectives can be co-optimized. A cluster of six computers is used to parallelize antenna simulations. Simulations can be performed using NEC or the MOM code described in the next section.

III. Antenna Simulation Approach

Full-wave simulation is used to estimate the performance of different antenna designs within the GA optimizer. For antennas consisting of metal wires or tubing, a wire code such as NEC provides good accuracy and fast run-time. For antennas

consisting of planar elements such as the blade antenna, it has been found that NEC provides reasonable accuracy if a relatively dense grid of wires is used to model the element. However, with such a modeling approach, one must generally make a trade-off between accuracy (particularly at higher frequencies) and run-time. In an optimization scheme such as GA where thousands of executions of the simulation code are necessary to achieve a solution, fast run-time is required. Wire-grid models also lack flexibility in that small physical features (relative to the size of the antenna) cannot be modeled.

An alternate Method of Moments (MOM) simulation code has been developed at the University of Texas, Austin for use in analyzing planar antennas. This code (here termed the "patch" code), which uses triangular facets to discretize a planar surface, is based upon the MOM formulation described in [5]. As shown in [5], the basis functions used require relatively few unknowns to accurately model the current distribution on a planar surface. Capabilities have been added to this code in order to analyze antennas including different feed excitation models, different ground models (PEC and lossy), radiation pattern calculation, and current visualization. An example meshing for the "large blade" antenna that would be used with this code is shown in Figure 1.

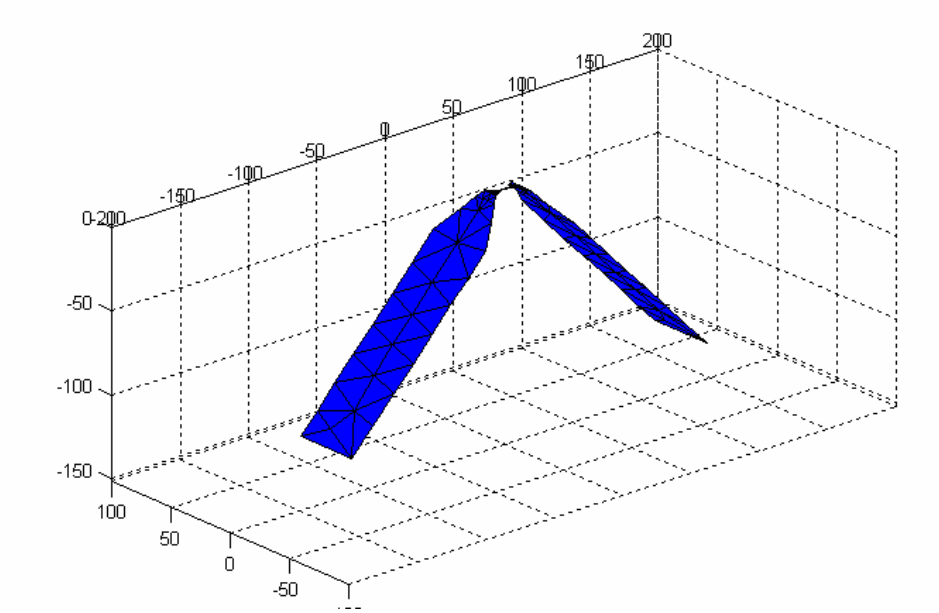

Fig. 1. A meshing of the large blade dipole for use with the patch code.

The simulated input impedance of the large blade antenna generated by this code is compared to simulation results from NEC and CST Microwave in Figure 2; the CST results were provided by N. Paravastu of NRL. Only the radiating elements, and not any mounting structure, are modeled in these simulations. In all simulations, an "average" ground with $\varepsilon_r = 13$, and $\sigma = 0.005$ is assumed. A measurement of the impedance of a large blade over a gravel ground provided by H. Schmitt of NRL is also included in the figure for comparison. All four results agree well all lower frequencies (40 MHz and below) and higher frequencies (80 MHz and up), but there are some discrepancies at intermediate frequencies, about the full-wave resonance of the antenna. The patch code

and CST results agree nearly perfectly across the entire frequency range except for some small ripples in the CST result. The peak impedance given by NEC is lower in amplitude and shifted down in frequency compared with the patch code and CST. Some error should be expected in the NEC simulation since a wire mesh can only roughly approximate a planar surface. The peak impedance from measurement happens to agree better with NEC, though it is shifted up in frequency compared with all of the simulation results. It is unclear what the cause of this discrepancy between CST / patch code results and measurement. Perhaps the permittivity and/or conductivity of the surface over which measurements were made are lower than the average ground assumed in simulation; this would have the effect of lowering the peak impedance. At the very least, the patch code appears to provide a reasonable approximation of the impedance of planar dipole antennas.

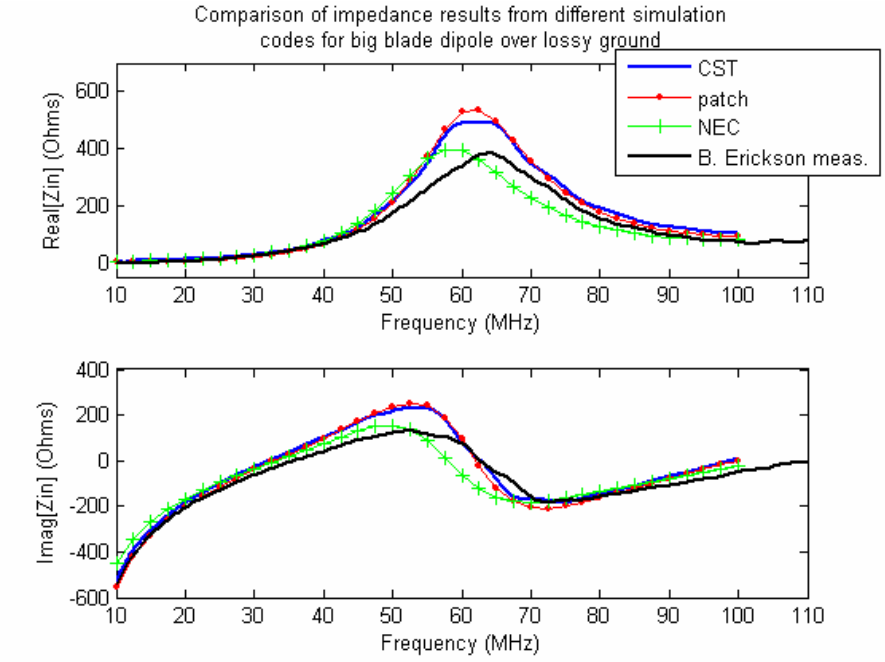

Fig. 2. Comparison of input impedance results for the large blade dipole from NEC, patch code, and CST simulations assuming an average lossy ground, and measurement over a gravel ground.

The simulated radiation patterns of the large blade dipole at 80 MHz generated by the patch code and NEC are compared in Figure 3. Overall, the agreement between the results is good, though some discrepancy is noted in the gain at lower elevation angles. This is likely due to the shift in frequency response between the two simulation results, which is evident in Figure 2. This frequency shift will modify the current distribution, which will in turn modify the radiation patterns.

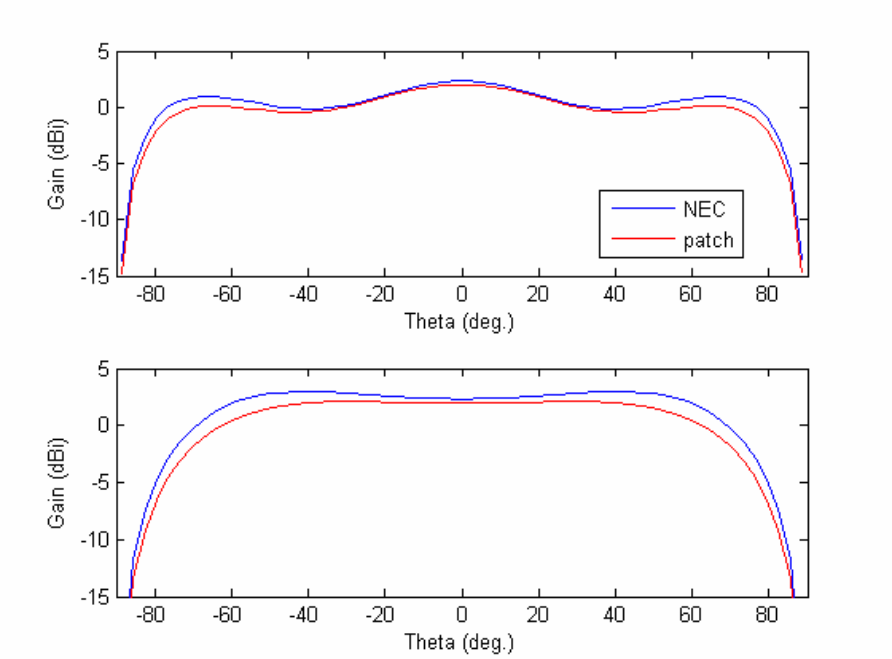

Fig. 3. Comparison of large blade dipole radiation patterns at 80 MHz generated by NEC and the patch code. (top) E-plane, (bottom) H-plane.

IV. Recent Results of Pareto GA Optimization of LWA Antennas

Work is underway to apply the Pareto GA optimizer described above to the problem of antenna design for the LWA. Antenna performance is optimized in terms of both sky noise performance and radiation pattern quality. Due to the nature of the Galactic Background spectra, very high effective antenna temperatures can be achieved at lower frequencies, while the antenna temperature at higher frequencies is limited by the rapidly declining background temperature. Therefore, it is desired to minimize losses at higher frequencies in order to maximize antenna temperature. One thought is that by compromising the antenna performance somewhat at lower frequencies, performance can be improved at higher frequencies. One way this could be achieved is to constrain the antenna temperature spectra to a profile T_g where at lower frequencies, a constant level, say 10 dB above system noise is maintained, but at higher frequencies the sky noise profile is closely followed; this is shown in Figure 4. The objective function used for sky noise performance in the GA is given by

$$F_1 = \sqrt{\frac{\sum_{\upsilon=1}^{N_\upsilon} w_\upsilon f(\upsilon)}{N}}$$

$$\text{where } f(\upsilon) = \begin{cases} (T_{ant}(\upsilon) - T_g(\upsilon))^2, & \text{if } T_{ant}(\upsilon) < T_g(\upsilon) \\ 0, & \text{if } T_{ant}(\upsilon) \geq T_g(\upsilon) \end{cases}$$

where $T_{ant}(\upsilon)$ is the effective sky noise temperature at the antenna terminals at frequency υ, N_υ is the number of frequencies, and w_υ is a weight which can be varied for each

frequency. Typically, higher frequencies are weighted more than lower frequencies since it is desired to achieve a good impedance match and low ground loss at higher frequencies. In the GA, the effective sky noise temperature at the antenna terminals is estimated using

$$T_{ant} = T_{sky}(1-|\Gamma|^2)\eta_{gnd},$$
$$\eta_{gnd} = \frac{P_{rad}}{P_{in}}$$

where T_{sky} is the galactic background spectra predicted by Cane's expression [6], $(1-|\Gamma|^2)$ is the mismatch loss of the antenna, and η_{gnd} is the ground efficiency of the antenna. The ground efficiency can be calculated exactly using the expression shown above, where P_{rad} is the total power radiated by the antenna which can be obtained by integrating the simulated far-field pattern over all observation angles above the ground, and P_{in}, the total input power, which can be calculated using the simulated input impedance.

The objective function for radiation pattern quality is

$$F_2 = \max_{all\,\upsilon}\left\{\sqrt{\frac{\sum_{i=1}^{N_\theta}\sum_{j=1}^{N_\phi}(G_{ant}(\upsilon,i,j)-G_{ref}(\upsilon,i,j))^2}{N_\theta N_\phi}}\right\}$$

which is simply the maximum over all frequencies of the rms error between the gain (or power) pattern of the designed antenna, G_{ant}, and a reference pattern, G_{ref}, over all observation angles. Though other pattern objective functions have been attempted in the GA, the rms pattern error objective function appears to work best. Typical reference power patterns used include $\sin(\theta)^2$ (Hertzian dipole), $\sin(\theta)$, and $\sin(\theta)^{1/2}$. These patterns give better results in the GA than a uniform pattern since they reflect the natural tendency of dipole patterns to roll-off at the horizon when operated over a ground.

Results from a recent GA execution are now presented. In this GA execution, blade-like dipoles with the following design parameters were optimized:

- element length and width,
- element taper length and angle,
- element bend point and angle,
- feed spacing, and
- antenna height.

These parameters were allowed to vary over a relatively wide range so that performance trade-offs could be explored more thoroughly. For instance, the maximum element width could vary between 25 and 55 cm, the total element length could vary between 45 and 320 cm, and antenna height could vary between 50 and 220 cm. However, some constraints were enforced explicitly in the GA to maintain realizable designs. These include constraining the bent portion of the antenna so that it does not extend below ground (with a 3 inch clearance), and constraining the element dimensions such that

when two identical dipoles are placed orthogonal to each other, no portion of the elements will intersect (with a 1 cm clearance.) The reference sky noise profile shown in Figure 4 was used to optimize sky noise response. A system temperature of 250 K was assumed corresponding to a peak desired antenna temperature of 2500 K. Patterns were optimized using the sin(θ) reference power pattern. A lossy ground with $\varepsilon_r = 13$, and $\sigma = 0.005$ was assumed. Optimization was performed simultaneously over the entire frequency range of 20 MHz to 80 MHz.

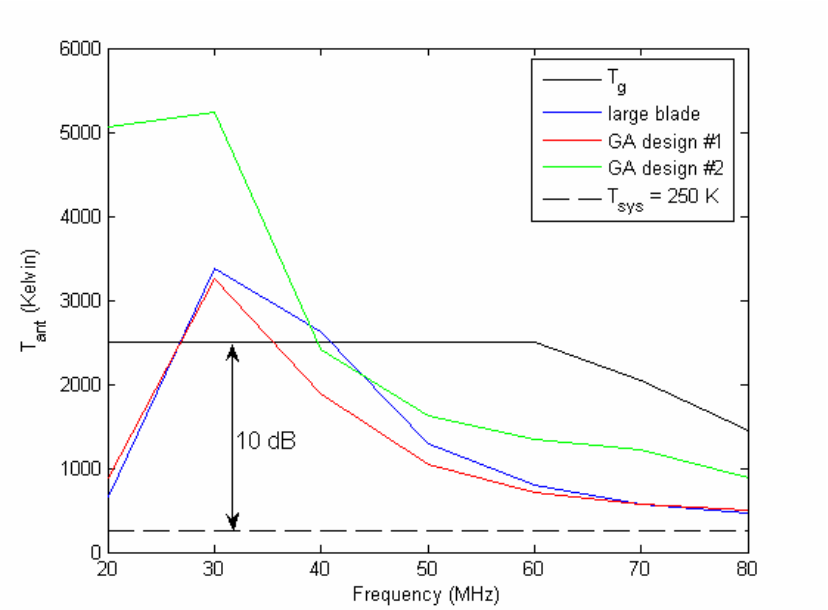

Figure 4. Effective temperature design profile (T_g) used in GA, effective temperature spectra of the large blade dipole and selected GA generated designs.

Figure 5 shows the performance of the GA in objective space (vertical axis = sky noise performance, horizontal axis = pattern quality). In the first generation, the population is spread randomly throughout objective space. However, as the optimization progresses, the population drifts inward, indicating improved antenna performance. After many generations, a distinct Pareto front begins to emerge, which denotes the "optimal" trade-off between sky noise performance and pattern quality; the front generated after generation 140 is shown in the figure. A high percentage of the population lies along the final Pareto front, and a wide range of objective function values are covered by the front. This demonstrates that the basic mechanics of the optimizer are functioning properly.

The results shown in Figure 5 indicate that a relatively wide range of trade-offs between sky noise performance and pattern quality can be achieved with blade-like dipole antennas. It is interesting to note that the large blade design falls relatively close to the final front, which indicates that it provides a nearly optimal performance trade-off near the lower end of the range of pattern objective function values (at least for the design parameter set considered here.) Two designs from the final front were selected for further analysis, and are circled in Figure 5. Design #1 (green circle), which is depicted in Figure 6, exhibits similar objective function values as the large blade. The total element length, 176 cm, and maximum width, 46 cm, of this design are very similar to

the large blade, though the bend point in this design is much further from the feed. Also, the element in this design is placed much closer to the ground, 85 cm, than the blade design, 150 cm. The sky noise spectra of design #1 is compared with that of the large blade and the design temperature profile in Figure 4. As can be seen, the sky noise spectra of the GA design is very similar to the large blade over the entire frequency range. The reduced height of the GA design leads to higher ground loss at lower frequencies. Moving the bend point out away from feed improves the impedance match at lower frequencies, however, which cancels the additional ground loss. The response of the large blade is slightly better at intermediate frequency which reflects the fact its sky noise objective function value is lower than the design #1 as seen in Figure 5. The radiation patterns of the two designs at 80 MHz (where they are expected to be at their worst) are compared in Figure 7. As expected, the GA design exhibits somewhat improved agreement with the reference pattern compared with the large blade. While some ripple is evident in the large blade design, none is evident in the GA design.

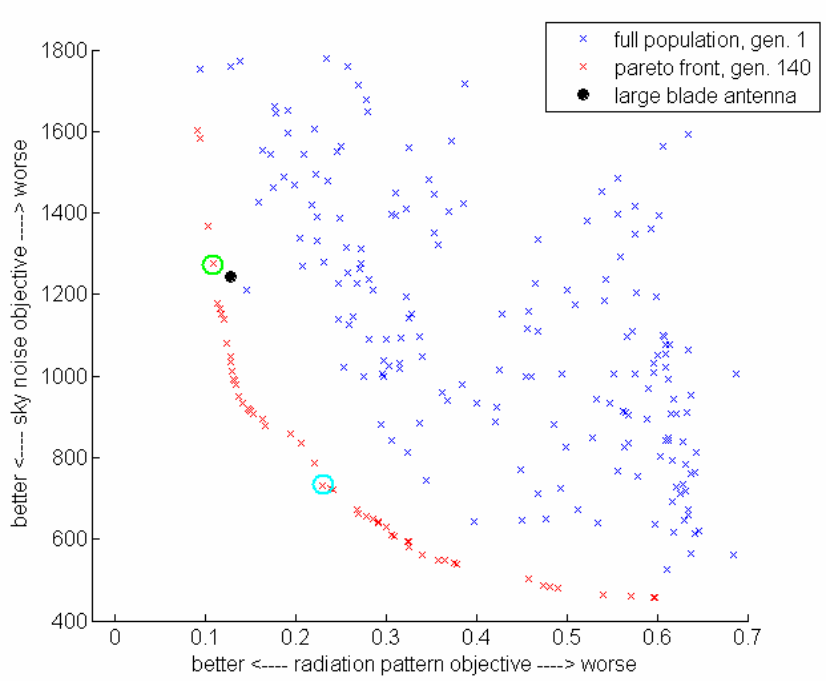

Figure 5. Scatter of population in objective space in generation 1 and the generated Pareto front after generation 140. The performance of the large blade antenna is shown for comparison. GA designs selected for analysis are circled in green (design #1) and cyan (design #2).

GA design #2 (cyan circle in Figure 5) is depicted in Figure 8. The total length of this design, roughly 226 cm, is much longer than the large blade. This length causes the second half-wave resonance of the antenna to occur near 80 MHz, which improves impedance matching at higher frequencies. Also, the maximum element width has been increased as far as possible to 55 cm. This will reduce the peak impedance, which improves matching at intermediate frequencies. Finally the antenna height is increased

relative to GA design #1 to 126 cm, which will improve impedance matching and reduce ground loss. All of these factors lead to an improved sky noise response as compared with design #1 and the large blade, which is evident in Figure 4. This improvement in sky noise response comes at the expense of pattern quality, however, as seen in Figure 7. Compared with the other two designs, Design #2 exhibits higher ripple in its radiation patterns, and has lower gain at lower elevation angles in the E-plane at 80 MHz. This trend of improving sky noise response with degrading pattern quality will continue as one moves left to right on the Pareto front in Figure 5.

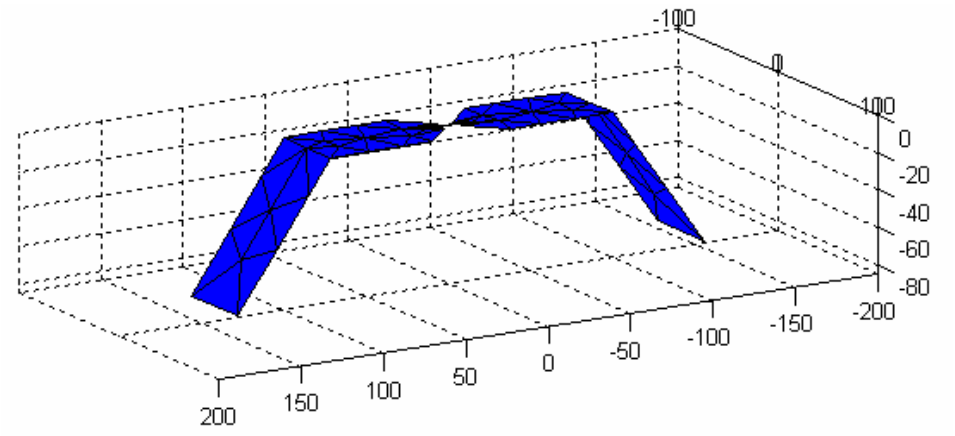

Figure 6. Design #1 (better patterns) from final Pareto front.

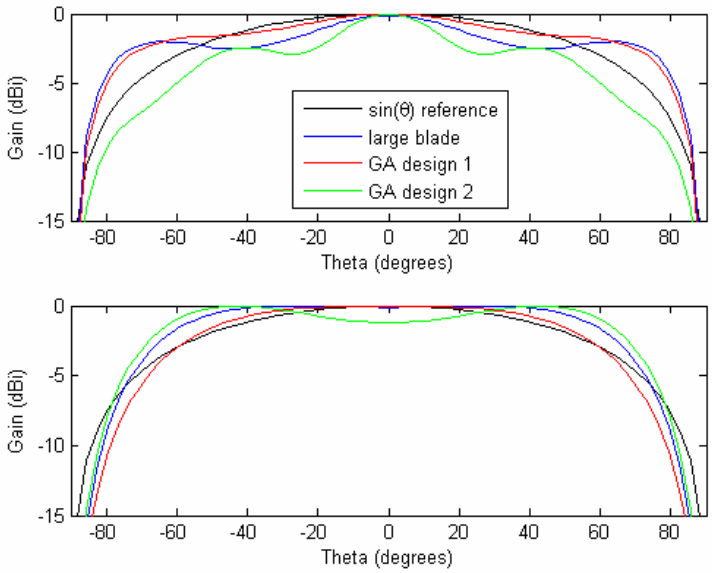

Figure 7. Radiation patterns of selected GA designs at 80 MHz. E-plane (top), H-plane (bottom.)

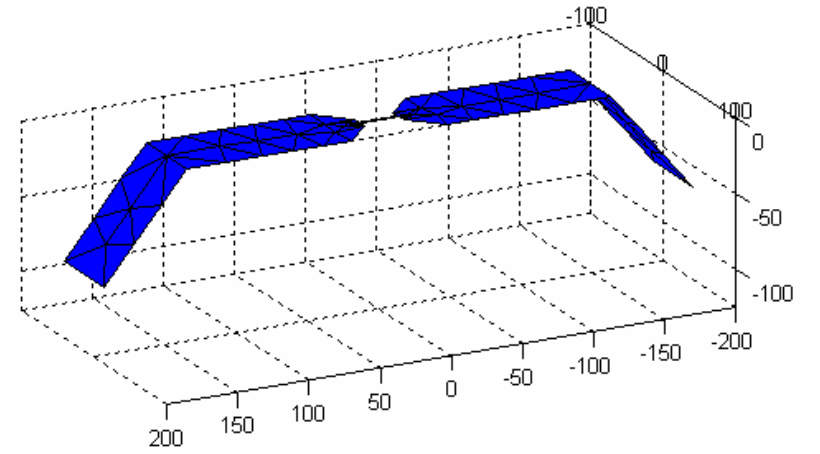

Figure 8. Design #2 (better sky noise response) from final Pareto front.

V. Upcoming Work

There are a number of cases that are planned for study using the Pareto GA optimizer. The design parameter set will be augmented to determine if improved performance can be achieved as compared with Figure 5. This will include adding additional edge tapers and element bends to the basic blade dipole parameter set. The radiating element may also be flipped on edge (similar to the NLTA dipole antenna), which will allow wider elements to be used (which will improve impedance matching) without the risk of intersection between orthogonal dipoles. The improvement offered by ground reflectors will also be studied using the GA. This will first be approximated using an infinite PEC ground since this leads to very fast run-times. Then finite-sized metal plates (the patch code models plates much more efficiently that wire meshes) will be co-optimized with the radiating element. Additionally, some work will be done to determine if different reference sky noise spectra profiles (compared the reference profile depicted in Figure 4) lead to improved performance. In early GA executions, design parameter values will be allowed to vary over a wide range in order to thoroughly explore the available performance trade-offs. After these results have been considered and performance and cost goals have been refined, the GA can be executed again with more tightly constrained parameter values in order to realize more practical and low-cost antenna designs. It is currently planned to construct low-cost prototypes of the most promising designs, and perform measurements in order to validate the results of the optimizer.

VI. Summary

The expected result from this effort is a series of Pareto fronts which describe the optimal performance trade-off between sky noise response and radiation pattern quality that can be achieved with a number of different planar dipole antenna topologies. These fronts can serve as design curves, which should greatly aid in designing planar dipoles for use in LWA. It is expected that at least somewhat better performance can be achieved

with planar dipoles as compared with dipole designs utilizing metal wires or tubing. Therefore the Pareto fronts for planar dipole performance can also serve as performance bounds for other antenna types, which would aid in the design of those antennas as well.

It should be noted that the Pareto GA optimizer described above is already capable of using the NEC code in addition to the patch code for simulation. Therefore, little additional effort would be required to apply the GA to other types of antennas currently being considered for LWA, which consist of wire or tubular elements.

References

[1] P. Ray, et al., "A strawman design for the Long Wavelenth Array stations", *LWA memo #35*, April 2006.

[2] A. Kerkhoff, R. Rogers, and H. Ling, "Design and analysis of planar monopole antennas using a genetic algorithm approach," *IEEE Trans. Antennas Propagat.*, vol. 52, pp. 2709-2718, Oct. 2004.

[3] A. Kerkhoff and H. Ling, "Design of band-notched planar monopole antenna using genetic algorithm optimization," accepted for publication in IEEE Trans. Antennas Propagat., early 2007.

[4] Y. Rahmat-Samii and E. Michielssen, *Electromagnetic Optimization by Genetic Algorithms*. New York: Wiley, 1999.

[5] L. Trintinalia, and H. Ling, "First order triangular patch basis functions for electromagnetic scattering," *J. of Electromagn. Waves and Appl.*, vol. 15, no. 11, p. 1521-1537, Nov. 2001.

[6] Cane, H.V., "Spectra of the Non-Thermal Radio Radiation from the Galactic Polar Regions," *MNRAS*, Vol. 189, p. 465, 1979.